

# Ellipsoidal collapse and previrialization

A. Del Popolo<sup>1,2,3</sup> and Z. Xia<sup>4</sup>

*Dipartimento di Matematica, Università Statale di Bergamo, Piazza Rosate, 2 - I 24129  
Bergamo, ITALY*

*Feza Gürsey Institute, P.O. Box 6 Çengelköy, Istanbul, Turkey*

*Boğaziçi University, 80185 Bebek, Istanbul, Turkey*

*CORA, Department of Applied Mathematics, Dalian University, Dalian 116024, China*

## ABSTRACT

We study the non-linear evolution of a dust ellipsoid, embedded in a Friedmann flat background universe, in order to determine the evolution of the density of the ellipsoid as the perturbation to it related detaches from general expansion and begins to collapse. We show that while the growth rate of the density contrast of a mass element is enhanced by the shear in agreement with Hoffman (1986a), the angular momentum acquired by the ellipsoid has the right magnitude to counterbalance the effect of the shear. The result confirms the previrialization conjecture (Peebles & Groth 1976; Davis & Peebles 1977; Peebles 1990) by showing that initial asphericities and tidal interactions begin to slow down the collapse after the system has broken away from the general expansion.

*Subject headings:* cosmology: theory—galaxies: formation

## 1. Introduction

While cosmologists generally believe that structures in the universe grew by gravitational instability from smaller inhomogeneities present at the epoch of decoupling, there is disagreement on several details of the model. One of these is the role of asphericity in the collapse of perturbations and structure formation.

According to the previrialization conjecture (Peebles & Groth 1976, Davis & Peebles 1977, Peebles 1990), initial asphericities and tidal interactions between neighboring density fluctuations induce significant non-radial motions which oppose the collapse. This means that virialized clumps form later, with respect to the predictions of the linear perturbation theory or the spherical collapse model, and that the initial density contrast, needed to obtain a given

final density contrast, must be larger than that for an isolated spherical fluctuation. This kind of conclusion was supported by Barrow & Silk (1981), Szalay & Silk (1983), Villumsen & Davis (1986), Bond & Myers (1993a,b) and Lokas et al. (1996).

In particular Barrow & Silk (1981) and Szalay & Silk (1983) pointed out that non-radial motions would slow the rate of growth of the density contrast by lowering the peculiar velocity and suppress collapse once the system detaches from general expansion. Villumsen & Davis (1986) gave examples of the growth of non-radial motions in N-body simulations. Arguments based on a numerical least-action method lead Peebles (1990) to the conclusion that irregularities in the mass distribution, together with external tides, induce non-radial motions that slow down the collapse. Lokas et al. (1996) used N-body simulations and a weakly non-linear perturbative approach to study previrialization. They concluded that when the slope of the initial power spectrum is  $n > -1$ , non-linear tidal interactions slow down the growth of density fluctuations and the magnitude of the effect increases when  $n$  is increased.

Opposite conclusions were obtained by Hoffman (1986a,1989), Evrard & Crone (1992), Bertschinger & Jain (1994) and Monaco (1995). In particular Hoffman (1986a,1989), using the quasi-linear (QL) approximation (Zel'dovich 1970; Zel'dovich & Novikov 1983) showed that the shear affects the dynamics of collapsing objects and it leads to infall velocities that are larger than in the case of non-shearing ones. Bertschinger & Jain (1994) put this result in theorem form, according to which spherical perturbations are the slowest in collapsing. The N-body simulations by Evrard & Crone (1992) did not reproduce previrialization effect, but the reason is due to the fact that they assumed an  $n = -1$  spectrum, differently from the  $n = 0$  one used by Peebles (1990) that reproduced the effect. If  $n < -1$  the peculiar gravitational acceleration,  $g \propto R^{-(n+1)/2}$ , diverges at large  $R$  and the gravitational acceleration moves the fluid more or less uniformly, generating bulk flows rather than shearing motions. Therefore, its collapse will be similar to that of an isolated spherical clump. If  $n > -1$ , the dominant sources of acceleration are local, small-scale inhomogeneities and tidal effects will tend to generate non-radial motions and resist gravitational collapse.

In a more recent paper, Audit et al. (1997) have proposed some analytic prescriptions to compute the collapse time along the second and the third principal axes of an ellipsoid, by means of the 'fuzzy' threshold approach. They point out that the formation of real virialized clumps must correspond to the third axis collapse and that the collapse along this axis is slowed down by the effect of the shear rather than be accelerated by it, in contrast to its effect on the first axis collapse. They conclude that spherical collapse is the fastest, in disagreement with Bertschinger & Jain's theorem. This result is in agreement with Peebles (1990).

In this paper, we address this controversy by following the evolution of a dust ellipsoid

in an expanding universe. We shall use a model of Nariai & Fujimoto (1972), that makes possible to study separately the effect of the shear,  $\Sigma$ , and that of angular momentum,  $L$ , on the protostructure evolution.

The paper is organized as follows. In section 2, we describe the model used; in section 3 we calculate the angular momentum of the ellipsoid at an intermediate time between the turn-around of the first and third axis, and in section 4 we describe the parameters and initial conditions used. Section 5 is devoted to the discussion of results and section 6 to conclusions.

## 2. Ellipsoid model for the collapse

In order to determine the evolution of the density in an ellipsoid of ideal fluid at zero pressure, we follow Nariai & Fujimoto (1972) and Barrow & Silk (1981). In what follows, we shall study the evolution of the density,  $\rho$ , of an ellipsoid embedded in a pressureless background cosmology with zero curvature characterized by a background density,  $\rho_b$ , and expansion parameter  $a(t)$ :

$$\rho_b = \frac{1}{6\pi G t^2} \quad a \propto t^{2/3} \quad (1)$$

As showed by Nariai & Fujimoto (1972), performing two transformations of coordinates from the co-moving frame  $\{\hat{x}^\mu\}$  to the inertial frame  $x^\mu = (t, x^i)$  with:

$$x^i = a(t)\hat{x}^i \quad (2)$$

and then from the last to a non-inertial system of reference,  $\{x'^\mu\}$ , rotating with angular velocity  $\Omega_i$  with respect to the inertial frame  $\{x^i\}$ , the Newtonian hydrodynamical equations of continuity, motion and Poisson are:

$$\frac{d\rho}{dt} + \frac{\partial V'_i}{\partial x'_i} \rho = 0 \quad (3)$$

$$\frac{dV'_i}{dt} + 2\varepsilon_{ijk}\Omega_j V'_k = \frac{1}{\rho} \frac{\partial p}{\partial x'_i} - \frac{\partial \phi}{\partial x'_i} - \left[ \left( \frac{4\pi G}{3} \rho_b - \Omega^2 \right) \delta_{ij} + \Omega_i \Omega_j - \varepsilon_{ijk} \frac{d\Omega_k}{dt} \right] x'_j \quad (4)$$

$$\nabla^2 \phi = 4\pi G(\rho - \rho_b) \quad (5)$$

where  $\rho$  and  $p$  are the density and pressure perturbations and (henceforth designating  $x'_i$  and  $V'_i$  with  $x_i$  and  $V_i$ , respectively):

$$\frac{d}{dt} \equiv \partial_t + V_i \frac{\partial}{\partial x_i} \quad (6)$$

Considering a rotating ellipsoid having uniform density,  $\rho = \rho(t)$ , the velocity field is given by:

$$V_i = \alpha_{ij}x_j \quad (7)$$

with:

$$\alpha_{ij} = \left[ \frac{1}{3} \left( \frac{\dot{\alpha}_1}{\alpha_1} + \frac{\dot{\alpha}_2}{\alpha_2} + \frac{\dot{\alpha}_3}{\alpha_3} \right) \delta_{ij} + \Sigma_{ij} + \varepsilon_{ijk}\omega_k \right] \quad (8)$$

where the shear tensor,  $\Sigma_{ij}$ , and the vorticity vector,  $\omega_k$ , are respectively given by:

$$\Sigma_{ij} \equiv \frac{1}{2} (\alpha_{ij} + \alpha_{ji}) - \frac{1}{3} \alpha_{kk} \delta_{ij} \quad (9)$$

$$\omega_i \equiv \varepsilon_{ijk} \alpha_{jk} \quad (10)$$

The term  $\alpha_i$  represent the  $i$  –  $th$  principal semi-axis of the ellipsoid. Assuming that the rotation velocity possesses only an  $x_3$  component and that the initial vorticity (note that here the term 'initial vorticity' shall not be interpreted as primordial vorticity, which is zero before orbit crossing, but as the vorticity acquired after shell-crossing) has no components in the directions of  $x_1$  and  $x_2$ , then the equations of motion for the principal axes of the ellipsoid and that for the evolution of density are:

$$\ddot{\alpha}_1 = -\frac{4\pi G}{3} \rho_b \left( 1 - \frac{3}{2} \alpha_1 \alpha_2 \alpha_3 U_1 \right) \alpha_1 - \frac{3}{2} GMU_1 \alpha_1 + \frac{8L^2}{(\alpha_1 + \alpha_2)^3} \quad (11)$$

$$\ddot{\alpha}_2 = -\frac{4\pi G}{3} \rho_b \left( 1 - \frac{3}{2} \alpha_1 \alpha_2 \alpha_3 U_2 \right) \alpha_2 - \frac{3}{2} GMU_2 \alpha_2 + \frac{8L^2}{(\alpha_1 + \alpha_2)^3} \quad (12)$$

$$\ddot{\alpha}_3 = -\frac{4\pi G}{3} \rho_b \left( 1 - \frac{3}{2} \alpha_1 \alpha_2 \alpha_3 U_3 \right) \alpha_3 - \frac{3}{2} GMU_3 \alpha_3 \quad (13)$$

$$\frac{\ddot{\rho}}{\rho} - \frac{4}{3} \left( \frac{\dot{\rho}}{\rho} \right)^2 - 4\pi G \rho - \Sigma^2 + \frac{8L^2}{\alpha_1 \alpha_2 (\alpha_1 + \alpha_2)^2} = 0 \quad (14)$$

(Nariai & Fujimoto 1972; Barrow & Silk 1981), where  $L$  is the angular momentum of the ellipsoid

$$U_i = \int_0^\infty \frac{dx}{(\alpha_i^2 + x)\psi^{1/2}(x)} \quad (15)$$

$$\psi(x) = \prod_{i=1}^3 (\alpha_i^2 + x) \quad (16)$$

$$M = \frac{4\pi}{3} \rho \alpha_1 \alpha_2 \alpha_3 = \text{constant} \quad (17)$$

and

$$\Sigma^2 = \sum_{i=1}^3 \Sigma_i^2 = \Sigma_1^2 + \Sigma_2^2 + \Sigma_3^2 \quad (18)$$

(see equation (3.22) of Nariai & Fujimoto (1972)). Equation (14), even if not strictly necessary to describe the evolution of the ellipsoid, is very useful because it allows us to qualitatively understand how the gravitational instability process is modified by the rotation and shear anisotropy. If  $\Sigma = L = 0$ , we are reconducted to the spherically symmetric case of no rotation. In this case the density reaches a maximum value of  $9\pi^2/16\rho_b$  and after the system recollapses. The shear,  $\Sigma^2$ , acts in the same sense of gravity making collapse easier, while the angular momentum  $L$  acts in the opposite sense to self-gravity,  $G\rho$ , making it easier to resist gravitational collapse. Obviously equation (14) could be also used to obtain the evolution of the density after calculating  $\Sigma^2$ , and  $L^2$ . As shown by Nariai & Fujimoto (1972),  $\Sigma^2$  is given by equation (18) and  $\Sigma_i$  can be obtained by means of equation (9) and equation (3.4) of Nariai & Fujimoto (1972) as follows:

$$\Sigma_i \equiv \Sigma_{ii} = \frac{1}{3} \left( 2 \frac{\dot{\alpha}_i}{\alpha_i} - \frac{\dot{\alpha}_j}{\alpha_j} - \frac{\dot{\alpha}_k}{\alpha_k} \right) \quad (19)$$

This last result shows even clearly that equation (11, 12, 13) form a closed system of equations giving the evolution of the ellipsoid and the shear.

Then the evolution of the density can be obtained (once the angular momentum is known) in two ways:

- 1) by integrating equation (11, 12, 13) to get the evolution of the semi-axes. Then  $\Sigma^2$  can be calculated through equation (19) and equation (18) and finally the density evolution is obtained by integrating equation (14).
- 2) By integrating equation (11, 12, 13) to get the evolution of the semi-axes and then using equation (17).

It is useful to remark that while the procedure 2) is simpler than 1) in the case  $\Sigma \neq 0$ , in the case  $L = \Sigma = 0$ , it is simpler to use the procedure 1) because, in this case, we *a priori* know that  $\Sigma = 0$  and consequently we have only to perform the integration of equation (14). If, otherwise, we wanted to use the procedure indicated in the point 2) we should integrate equation (11, 12, 13) and also impose the condition that  $\Sigma^2 = 0$  using equation (19), with a consequent complication of the calculations. In any case, in the paper, we performed the calculations following both the procedures, in order to check the consistency of the results.

A fundamental point to remark is the following: the Nariai & Fujimoto (1972) equations give a description of the evolution and collapse of an ellipsoid only if the ellipsoid has acquired somehow angular momentum. For the reasons described in the following, we use this model

to study the evolution of the ellipsoid from the epoch of turn-around of the first axis on.

An ellipsoid can have angular momentum for two different reasons:

1) the axes of the ellipsoid and that of the shear of the velocity field have an appropriate misalignment, or in other terms the principal axes of the inertia tensor are not aligned with the principal axes of the deformation tensor (see Catelan & Theuns 1996a,b). In this case, the ellipsoid can have angular momentum even if vorticity is zero. We are not interested in this particular case.

2) the system has a non-zero vorticity. Unfortunately, we now that according to Kelvin’s theorem, if the initial velocity field is irrotational, i.e. curl-free, then, it should remain irrotational also in the nonlinear regime. However, since the collapse of a protostructure is a violent phenomenon, the conditions of Kelvin’s circulation theorem should be violated (Chernin 1970). Then, there are two possibility for vorticity generation (see Sasaki & Kasai 1997):

a) acquisition of vorticity by the formation of shock fronts in the protostructure (pancake), in correspondence of shell-crossing (Doroshkevich 1970). Analytical studies by Pichon & Bernardeau (1999) have also shown that vorticity generation becomes significant at the scales  $3 - 4h^{-1}\text{Mpc}$ , and increases with decreasing scale;

b) acquisition of angular momentum by means of the tidal torques (Hoyle, 1949; Peebles 1969; Hoffman 1986b; Ryden & Gunn 1987). Current analytical description of vorticity and spin growth by tidal torques turn out to depend on a free parameter, i.e. the time when tidal torques cut off. This parameter has been related to either the beginning of the decoupling from the Hubble flow ( $\delta \simeq 1$ ) or the turn-around epoch (time when expansion halts) (for the spherical collapse model) (Andriani & Caimmi 1994). Numerical simulations (Barnes & Efstathiou 1987) have shown that after decoupling from the Hubble flow there are no substantial increment in angular momentum.

Summarizing, we know (and assume) that from the linear phase to shell-crossing the vorticity is zero, the ellipsoid has no rotation. The perturbation is subject to the gravitational field of matter inside the ellipsoid, which tends to make it collapse to a pancake, and to the tidal field of the matter outside, which cancels the effects of the interior gravitational field. As a result, the ellipsoid expands with the rest of the universe and preserves its shape until it enters the nonlinear phase (Barrow & Silk 1981; White & Silk 1979). When it reaches a density contrast  $\delta \simeq 1$  it detaches from Hubble expansion, and the distribution of matter of the ellipsoid tends to develop nonradial motions (Peebles 1980), (even if the axes of the ellipsoid and that of the shear of the velocity field have not an appropriate misalignment).

To take account of the rotation acquired, we identify the final angular momentum of the ellipsoid with that acquired at the maximum of expansion of the object (Peebles 1969;

Catelan & Theuns 1996a,b).

This assumption is justified by the fact that after the maximum expansion time the angular momentum stops growing, becoming less sensitive to tidal couplings (Peebles 1969; Barnes & Efstathiou 1987).

In other words, we assume that the total angular momentum is acquired before the ellipsoid collapse, since the tidal torques are much less effective afterwards (Peebles 1969; Catelan & Theuns 1996a,b). While for a spherical perturbation this time is well defined (it is the turn-around epoch), for an aspherical perturbation this epoch is not well defined and the system should be followed until the long axis turns around (Eisenstein & Loeb 1995), since the acquisition of angular momentum is important until the collapse of this axis. To simplify things, we choose a mean value of time,  $t_M$ , between the turnaround of the shortest axis and that of the longest (see Hoffman 1986b)

### 3. Angular momentum at $t_M$

As previously remarked, if we want that equation (11, 12, 13) constitute a closed system of equations to get the ellipsoid evolution, we need the angular momentum  $L$ . As stressed previously, we need only the value of the angular momentum of the virialized structure, that can be well approximated (see the above discussion) by its value at the time  $t_M$ .

The effect of tidal torques on structures evolution has been studied in several papers especially in connection with the origin of galaxies rotation. The explanation of galaxies spins gain through tidal torques was pioneered by Hoyle (1949) in the context of a collapsing protogalaxy. Peebles (1969) considered the process in the context of an expanding world model, showing that the angular momentum gained by the matter in a random comoving *Eulerian* sphere grows at the second order in proportion to  $t^{5/3}$  (in a Einstein-de Sitter universe), since the proto-galaxy was still a small perturbation, while in the non-linear stage the growth rate of an oblate homogeneous spheroid decreases with time as  $t^{-1}$ .

White (1984) considered an analysis by Doroshkevich (1970) that showed that the angular momentum of galaxies grows to first order in proportion to  $t$  and that Peebles's result is a consequence of the spherical symmetry imposed to the model. White showed that the angular momentum of a Lagrangian sphere does not grow either in the first or in the second order, while the angular momentum of a non-spherical volume grows to the first order in agreement with Doroshkevich's result.

Another way to study the acquisition of angular momentum by a proto-structure is that followed by Ryden (1988) (hereafter R88) and Eisenstein & Loeb (1995). Following Eisen-

stein & Loeb (1995), we separate the universe into two disjoint parts: the collapsing region, characterized by having high density, and the rest of the universe. The boundary between these two regions is taken to be a sphere centered on the origin. As usual, in the following, we denote with  $\rho(\mathbf{x})$ , being  $\mathbf{x}$  the position vector, the density as function of space and  $\delta(\mathbf{x}) = \frac{\rho(\mathbf{x}) - \rho_b}{\rho_b}$ . The gravitational force exerted on the spherical central region by the external universe can be calculated by expanding the potential,  $\Phi(\mathbf{x})$ , in spherical harmonics. Assuming that the sphere has radius  $R$ , we have:

$$\Phi(\mathbf{x}) = \sum_{l=0}^{\infty} \frac{4\pi}{2l+1} \sum_{m=-l}^l a_{lm}(x) Y_{lm}(\theta, \phi) x^l \quad (20)$$

where  $Y_{lm}$  are spherical harmonics and the tidal moments,  $a_{lm}$ , are given by:

$$a_{lm}(x) = \rho_b \int_R^{\infty} Y_{lm}(\theta, \phi) \rho(\mathbf{s}) s^{-l-1} d^3s \quad (21)$$

In this approach the proto-structure is divided into a series of mass shells and the torque on each mass shell is computed separately. The density profile of each proto-structure is approximated by the superposition of a spherical profile,  $\delta(r)$ , and the same Gaussian density field which is found far from the peak,  $\varepsilon(\mathbf{r})$ , which provides the quadrupole moment of the proto-structure. To the first order, the asphericity about a given peak can be represented writing the initial density in the form:

$$\rho(\mathbf{r}) = \rho_b [1 + \delta(r)] [1 + \varepsilon(\mathbf{r})] \quad (22)$$

(Ryden & Gunn 1987; R88; Peebles 1980, equation (18.5)) where  $\varepsilon(\mathbf{r})$  satisfies the following equations:

$$\langle |\varepsilon_k|^2 \rangle = P(k) \quad (23)$$

being  $P(k)$  the power spectrum, and:

$$\langle \varepsilon(\mathbf{r}) \rangle = 0, \quad \langle \varepsilon(\mathbf{r})^2 \rangle = \xi(0) \quad (24)$$

(Ryden & Gunn 1987; Peebles 1980), where  $\langle \rangle$  indicates a mean value of the physical quantity considered and  $\xi$  the two-point correlation function (note that the previous equations are obtained in the lowest order approximation. The limits of the same are described in Ryden & Gunn 1987). The torque on a thin spherical shell of internal radius  $x$  is given by:

$$\tau(x) = -\frac{GM_{sh}}{4\pi} \int \varepsilon(\mathbf{x}) \mathbf{x} \times \nabla \Phi(\mathbf{x}) d\Omega \quad (25)$$

where  $M_{sh} = 4\pi\rho_b [1 + \delta(x)] x^2 \delta x$ . Before going on, I want to recall that we are interested in the acquisition of angular momentum from the inner region, and for this purpose we take



account only of the  $l = 2$  (quadrupole) term. In fact, the  $l = 0$  term produces no force, while the dipole ( $l = 1$ ) cannot change the shape or induce any rotation of the inner region. As shown by Eisenstein & Loeb (1995), in the standard CDM scenario the dipole is generated at large scales, so the object we are studying and its neighborhood move as bulk flow with the consequence that the angular distribution of matter will be very small, then the dipole terms can be ignored. Because of the isotropy of the random field,  $\varepsilon(\mathbf{x})$ , Equation (25) can be written as:

$$\langle |\tau|^2 \rangle = \sqrt{30} \frac{4\pi G}{5} \left[ \langle a_{2m}(x)^2 \rangle \langle q_{2m}(x)^2 \rangle - \langle a_{2m}(x) q_{2m}^*(x) \rangle^2 \right]^{1/2} \quad (26)$$

As stressed in the next section, following Eisenstein & Loeb (1995), the integration of the equations of motion shall be ended at some time before the inner external tidal shell (i.e., the innermost shell of the part of the universe outside the sphere containing the ellipsoid) collapses. Then the inner region behaves as a density peak. This last point is an important one in the development of the present paper.

An important question to ask, before going on, regards the role of triaxiality of the ellipsoid (density peak) in generating a quadrupole moment. Equation (26) takes into account the quadrupole moment coming from the secondary perturbation near the peak. The density distribution around the inner region is characterized (see Equation (22)) by a mean spherical distribution,  $\delta$ , and a random isotropic field. In reality the central region is a triaxial ellipsoid. It is then important to evaluate the contribution to the quadrupole moment due to the triaxiality. Remembering that the quadrupole moments are given by:

$$q_{2m} = \int_{|\mathbf{r}| < R} Y_{2m}^*(\theta, \phi) s^2 \rho(\mathbf{s}) d^3 s = \frac{x^2 M_{\text{sh}}}{4\pi} \int Y_{2m}^*(\theta, \phi) \varepsilon(\mathbf{x}) d\Omega \quad (27)$$

and approximating the density profile as:

$$\delta(\mathbf{x}) = \langle \delta(x) \rangle_{\text{spherical}} + \nu f(x) A(e, p) \quad (28)$$

being  $\langle \delta(x) \rangle_{\text{spherical}}$  the mean spherical profile,  $\nu = \frac{\delta}{\sigma}$  the peak height and  $\sigma$  the r.m.s. value of  $\delta$ . The function  $A(e, p)$  of the triaxiality parameters,  $e$  and  $p$ , is given by:

$$A(e, p) = 3e(1 - \sin^2 \theta - \sin^2 \theta \sin^2 \phi) + p(1 - 3 \sin^2 \theta \cos^2 \phi) \quad (29)$$

while the function  $f(x)$  is given (R88) by:

$$f(x) = \frac{5}{2\sigma} R_*^2 \left( \frac{1}{x} \frac{d\xi}{dx} - \frac{1}{3} \nabla^2 \xi \right) \quad (30)$$

where  $\xi$ ,  $\sigma$  and  $R_*$  are respectively the two-point correlation function, the mass variance and a parameter connected to the spectral moments (see Bardeen et al. 1986, equation (4.6d),

hereafter BBKS). Substituting equation (28) and equation (29) in equation (27) it is easy to show that the sum of the mean quadrupole moments due to triaxiality is:

$$\frac{1}{M_{\text{sh}}} \sum_{m=-2}^2 \langle q_{2m}(x) \rangle = \nu x^2 f(x) \left( \frac{1}{2\pi} \sqrt{6\pi/5}(e-p) + \frac{1}{4\pi} \sqrt{4\pi/5}(3e+p) \right) \quad (31)$$

which must be compared with that produced by the secondary perturbations,  $\varepsilon$ :

$$\langle q_{2m}(x)^2 \rangle = \frac{x^4}{(2\pi)^3} M_{\text{sh}}^2 \int k^2 P(k) j_2(kx)^2 dk \quad (32)$$

where  $j_2$  is the Bessel function of order 2. The values of  $e$  and  $p$  can be obtained from the distribution of ellipticity and prolateness (BBKS, equation (7.6) and figure 7) or for  $\nu > 2$  by:

$$e = \frac{1}{\sqrt{5}x [1 + 6/(5x^2)]^{1/2}} \quad (33)$$

and

$$p = \frac{6}{5x^4 [1 + 6/(5x^2)]^2} \quad (34)$$

(BBKS equation (7.7)), where  $x$  is given in BBKS (equation (6.13)). In the case of a peak with  $\nu = 3$ , we have  $e \simeq 0.15$ ,  $p \simeq 0.014$  while for peaks having  $\nu = 2$  and  $\nu = 1$  they are respectively given by  $e \simeq 0.2$ ,  $p \simeq 0.03$  and  $e \simeq 0.25$   $p \simeq 0.04$ .

As shown in figure 1, for a  $3\sigma$  profile, the source of quadrupole moment due to triaxiality is less important than that produced by the random perturbations  $\varepsilon$  in all the proto-structure, except in the central regions where the quadrupole moment due to triaxiality is comparable in magnitude to that due to secondary perturbations. In other words, the triaxiality has a significant effect only in the very central regions, which contains no more than a few percent of the total mass and where the acquisition of angular momentum is negligible. It follows that the triaxiality can be ignored while computing both expansion and spin growth (R88). Moreover, as observed by Eisenstein & Loeb (1995), the ellipsoid model does better in describing low shear regions (having higher values of  $\nu$ ), whose collapse is more spherical and then the effects of triaxiality are less evident. Just this peaks, having at least  $\nu > 2$ , shall be studied in this paper. In any case, even if the triaxiality was not negligible it should contribute to increment the acquisition of angular momentum (Eisenstein & Loeb 1995), and finally to a larger effect on the density evolution, (i.e., a larger reduction of the growing rate of the density).

In order to find the total angular momentum imparted to a mass shell by tidal torques, it is necessary to know the time dependence of the torque. This can be done connecting  $q_{2m}$  and

$a_{2m}$  to parameters of the spherical collapse model (Eisenstein & Loeb 1995 (equation (32), R88 (equation (32) and (34))). Following R88 we have:

$$q_{2m}(\theta) = \frac{1}{4} q_{2m,0} \bar{\delta}_0^{-3} \frac{(1 - \cos \theta)^2 f_2(\theta)}{f_1(\theta) - \left(\frac{\delta_0}{\bar{\delta}_0}\right) f_2(\theta)} \quad (35)$$

and

$$a_{2m}(\theta) = a_{2m,0} \left(\frac{4}{3}\right)^{4/3} \bar{\delta}_0 (\theta - \sin \theta)^{-4/3} \quad (36)$$

The collapse parameter  $\theta$  is given by:

$$t(\theta) = \frac{3}{4} t_0 \bar{\delta}_0^{-3/2} (\theta - \sin \theta) \quad (37)$$

Equation (35) and (36), by means of equation (26), give to us the tidal torque:

$$\tau(\theta) = \tau_0 \frac{1}{3} \left(\frac{4}{3}\right)^{(1/3)} \bar{\delta}_0^{-1} \frac{(1 - \cos \theta)^2}{(\theta - \sin \theta)^{(4/3)}} \frac{f_2(\theta)}{f_1(\theta) - \left(\frac{\delta_0}{\bar{\delta}_0}\right) f_2(\theta)} \quad (38)$$

where  $f_1(\theta)$  and  $f_2(\theta)$  are given in R88 (Eq. 31),  $\tau_0$  and  $\delta_0 = \frac{\rho - \rho_b}{\rho_b}$  are respectively the torque and the mean fractional density excess inside the shell, as measured at current epoch  $t_0$ . The angular momentum acquired during expansion can then be obtained integrating the torque over time:

$$L = \int \tau(\theta) \frac{dt}{d\theta} d\theta \quad (39)$$

As remarked in the previous section, the angular momentum obtained from equation(39) is evaluated at the time  $t_M$ . Then the calculation of the angular momentum can be solved by means of equation (39), once we have made a choose for the power spectrum. With the power spectrum and the parameters given in the next section and for a  $\nu = 2$  peak, the model gives a value of  $2.5 \times 10^{74} \text{gcm}^2/\text{s}$ .

Since the calculation of the angular momentum is fundamental for the evolution of the ellipsoid, it is worthwhile to comment on the validity of the calculation and the result.

To start with, we want to recall that, independently from the he calculation followed in order to get the angular momentum, we need only its final value. Then it is important to compare the result obtained with our approach with those obtained following different approaches. An interesting comparison is that with the result of Catelan & Theuns (1996a). In their paper, they calculated the angular momentum at maximum expansion time (see their equations (31)-(32)) and compared it with previous theoretical and observational estimates. Assuming the same value of mass  $\nu$  used to obtain our previously quoted result

( $2.5 \times 10^{74} \text{gcm}^2/\text{s}$ ) and the same value of redshift ( $z = 3$ ) and distribution of the final angular momentum  $l_f$  adopted by Catelan & Theuns (1996a), we get a value for the angular momentum of  $2 \times 10^{74} \text{gcm}^2/\text{s}$ . This last result is in good agreement with ours and is well in line with previous theoretical estimates (Peebles 1969; Heavens & Peacock 1988) and numerical simulations (Fall 1983). It is obvious that the approach of this paper or that of Catelan & Theuns (1996a) cannot predict the very final stages of evolution when clumps merge and interact non-linearly and in addition dissipative processes may play an important role as well. In any case, the value of the final angular momentum, as obtained from the extrapolation of the linear theory, is typically a factor of  $\simeq 3$  larger than the final spin of the non-linear object (Barnes & Efstathiou 1987; Frenk 1987). The effects of this discrepancy can be simply eliminated reducing the angular momentum by the same factor.

I want to remark that we have used some results of the random Gaussian fields in order to calculate the torque (e.g., equation (30)). This could seem a rather strong assumption, being us concerned with small scales, where the density field is no more Gaussian. This assumption is justified by what previously told, namely by the fact that our calculation of the final angular momentum is obtained as an extrapolation of the linear theory and as previously quoted this approach gives values of the angular momentum not too different from those obtained in numerical simulations.

As previously quoted, we assume that from  $t_M$  on, the ellipsoid has this constant angular momentum. Following the procedures 1) and/or 2), we shall be able to get the time evolution of the density and that of the collapse velocity.

#### 4. Parameters, constraints and initial conditions

In order to apply the model introduced in the previous section to the evolution of the collapsing perturbation and solve equations (11)–(14), we need the initial conditions and moreover it is necessary to connect this conditions and the time dependence of the shear to properties of the initial density field. To begin with, initially, the high density region that shall collapse has  $\delta \ll 1$ , and it is contained in a spherical region. Following Eisenstein & Loeb (1995), we impose that average mass, density and quadrupole moments of the ellipsoid match that of the inner spherical region at the initial time. So defining, as usual, the overdensity of the inner region as:

$$\bar{\delta}(R) = \frac{3}{R^3} \int_0^R \delta(y) y^2 dy \quad (40)$$

the mass of the region is given by:

$$M = \frac{4\pi}{3}\rho_b R^3 [1 + \bar{\delta}(R)] = \frac{4\pi}{3}\rho_b R^3 [1 + \nu\sigma] \quad (41)$$

The ellipsoid is chosen to match the previous quantities: it has overdensity  $\bar{\delta}(R)$ , mass,  $M = \frac{4\pi}{3}\rho_b [1 + \bar{\delta}(R)] \alpha_1 \alpha_2 \alpha_3$  and by comparison with equation (41) we get:

$$R^3 = \alpha_1 \alpha_2 \alpha_3 \quad (42)$$

The quadrupole moments, necessary to set  $q_{2m,0}$  in equation (35) are obtained from equation (27). The initial axes of the ellipsoid are fixed as follows: given a value of  $\delta$  (or  $\nu$ ) and the initial mass,  $M$ , we can calculate the radius  $R$  from equation (41). Equation (42), (33), (34) make possible to get  $\alpha_1, \alpha_2, \alpha_3$ . The initial density, for the case  $\nu = 2$ , is  $\delta = 2 \times 10^{-3}$ , and  $M \simeq 2 \times 10^{11} M_\odot$  (since we are concerned with galactic mass scales), and the velocity is chosen to be a uniform expansion with the Hubble flow (a pure growing mode).

The equations of the model described in section 2 were integrated using the Bulirsch-Stoer algorithm. We assumed an  $\Omega = 1$  universe, a Hubble constant of  $H_0 = 50 \text{ km/s/Mpc}$ . The CDM power spectrum that I adopt is  $P(k) = AkT^2(k)$  with the transfer function  $T(k)$  given in BBKS (equation (G3)):

$$T(k) = \frac{[\ln(1 + 2.34q)]}{2.34q} \cdot [1 + 3.89q + (16.1q)^2 + (5.46q)^3 + (6.71q)^4]^{-1/4} \quad (43)$$

where  $A$  is the normalizing constant and  $q = \frac{k\theta^{1/2}}{\Omega_x h^2 \text{Mpc}^{-1}}$ . Here  $\theta = \rho_{\text{er}}/(1.68\rho_\gamma)$  represents the ratio of the energy density in relativistic particles to that in photons ( $\theta = 1$  corresponds to photons and three flavors of relativistic neutrinos). The spectrum was smoothed on a galactic scale ( $R \simeq 0.5h^{-1} \text{ Mpc}$ ) and normalized such that  $\sigma(8h^{-1}\text{Mpc}) = 1$  at present epoch ( $\sigma_8$  is the rms value of  $\frac{\delta M}{M}$  in a sphere of  $8h^{-1}\text{Mpc}$ ). The mass variance present in equation (39) can be obtained from the spectrum,  $P(k)$ , as:

$$\sigma^2(R) = \frac{1}{2\pi^2} \int_0^\infty dk k^2 P(k) W^2(kR) \quad (44)$$

where  $W(kR)$  is a top-hat smoothing function:

$$W(kR) = \frac{3}{(kR)^3} (\sin kR - kR \cos kR) \quad (45)$$

The remaining spectral parameters of equation (39),  $\gamma, R_*$ , for the chosen spectrum with the above fixed smoothing length, are  $\gamma \simeq 0.6, R_* = 0.52$ . For what concerns the duration of

the integration, we followed the suggestions of Eisenstein & Loeb (1995): since the average overdensity of the innermost external shell is of the same order of magnitude of that of the ellipsoid, the two objects collapse at similar times, or in some cases the inner external shell collapses before the long axis of the ellipsoid. To avoid the problem, the integration must be stopped at some time before the collapse of the inner tidal shell. This can be accomplished (Eisenstein & Loeb 1995) by constraining the initial conditions so that none of the exterior shells has an overdensity greater than 95% of the initial density of the ellipsoid. The last assumption ensures that the external tidal shells does not collapse before the integration ends. As a consequence the inner region behaves as a density peak. We also imposed the condition  $\bar{\delta}(R_{\text{Sphere}}) > \nu\sigma$ , with  $\nu > 2$ , implying that the inner spherical region have high overdensity, and finally we follow Bond & Myers (1993a,b), imposing the condition that no axis may collapse below 40% of its maximum length, in order to avoid that the dynamics approaches the singularity at zero length and to simulate virialization of the corresponding axis.

## 5. Results

The results of the calculation involving the evolution of  $\delta$  are shown in figures 2-5.

In figure 2, we plot  $\delta = \frac{\rho - \rho_b}{\rho_b}$  in the case of a density peak having height  $\nu = \delta/\sigma(R) = 2$ . The solid line represents the solution of equation (14) in the case  $L = \Sigma = 0$ . The dashed and dotted lines representing the case  $L = 0, \Sigma \neq 0$  and  $L \neq 0, \Sigma \neq 0$ , respectively, were obtained using both the procedure 1) and 2) described in section 2. As shown, the shear (see dashed line) produces an enhancement of the growth rate of the density of a mass element. This is the growth rate enhancement of the density contrast effect induced by the shear firstly recognized by Hoffman (1986a). The shear term,  $\Sigma^2$ , appearing in the equation of evolution of the density (equation(14)) is positive definite, so as long as the fluid is irrotational, the growth rate of the density contrast must be enhanced by it, so the effects of the shear are present in the linear and nonlinear regime. During the linear phase the ellipsoid expands with the universe: the tidal field outside the ellipsoid cancels the effects of the gravitational field interior to it. The shear contributes to increase the growth rate of the perturbation. When the effect of the angular momentum can no longer be neglected, we see that the situation previously described changes (see dotted line). Initially the shear term dominates, but in a short time the angular momentum begins to influence the growth of the perturbation, counterbalancing the effect of the shear term,  $\Sigma^2$ , and producing a slowing down of the growth. As a final result the growth of the density perturbation becomes slower than in the

case  $L = \Sigma = 0$ . The density contrast at virialization,  $\delta_v \simeq 60$ , is reduced with respect to the expected value  $\delta_v \simeq 178$ . The value obtained is intermediate between that obtained by Peebles (1990) for the half-mass radius,  $\delta_v \simeq 30$ , and that obtained by the modified spherical collapse model of Engineer et al. (1998),  $\delta_v \simeq 80$ . We want to remark that in this last paper the authors showed that in order to take account of the effects coming from the asphericity of a system, one has to add to the equations for the density evolution typical of the spherical collapse model an additive term,  $(1 + \delta)(\Sigma^2 - 2\Omega^2)$ , depending on shear and angular momentum of the system, similarly to Nariai & Fujimoto (1972) model.

The previous result can be interpreted as follows: when the overdensity of the ellipsoid become considerable, and  $\delta$  attains amplitudes of order unity the ellipsoid will begin to recollapse in at least one direction. As shown by Peebles (1980), if we consider the collapse of the sphere of equivalent mass, when this reaches the turn-around epoch one of the axis of the ellipsoid turns shorter and collapse forming a pancake in which the barions shock and the dark matter goes through violent relaxation. In the process the ellipsoid develops nonradial motion. The angular momentum  $L$  present in equation (11)–(14) becomes not negligible and produces the slowing down of density growth shown in the figure.

In figure 3, we show the same calculation of figure 2, but now we have increased the value of the peak height,  $\nu = 2.5$ . As in the previous case, the shear term produces an enhancement of the growth rate of the density (dashed line), but this time the effect is smaller with respect to that shown in figure 2. This is due to the fact that the shear magnitude decreases with increasing peak height (see also Hoffman 1986a, Table 1). As in figure 2, the angular momentum acts in the opposite direction to that of shear, but this time its effect is reduced (dotted line) with respect to the case  $\nu = 2$  because of the well known  $L-\nu$  anticorrelation effect (Hoffman 1986b). The trend is confirmed by figure 4 representing the same calculations of the figures 2-3 but now in the case  $\nu = 3$ .

Summarizing, both  $L$  and  $\Sigma$  reduce their rate of growth with increasing  $\nu$ : rare density peaks are in general characterized by a low shear, and then the evolution of the perturbation tends to follow the results of the spherical model, when  $\nu$  increases, and as expected also the collapse shall be nearly spherical (Bernardeau 1994).

In order to study the effect of angular momentum and shear on the collapse velocity, we calculate the collapse velocity at the epoch of pancaking numerically solving the equations of motions for the principal axes of the ellipsoid. Using Barrow & Silk (1981) notation, we indicate with  $x_o X(t)$  and  $z_o Z(t)$ , the principal axes ( $x_o$  and  $z_o$  are the initial values of the axes). We solve equations (11)–(13) to calculate the collapse velocity down the shortest axis at the epoch of pancaking in the case of an oblate spheroid ( $\alpha_1 = \alpha_2 > \alpha_3$ ). This calculation is similar to that of Barrow & Silk (1981) with the difference that our approach is a numerical

one. Then the collapse velocity at pancaking is:

$$v_{z_p} = -z_o \dot{Z}_p(t) \quad (46)$$

(from here on the subscript p indicates that the quantity is evaluated at the pancaking time). The initial conditions are set similarly to section 4 and the equation are solved for several values of  $x_o$ , while  $z_o = 1$ . In figure 5, we plot  $\frac{v_{z_p}}{a_p r_p / a_p}$ , where  $r_p = r_o X_p$  is the pancake radius (see Barrow & Silk 1981), as function of the ratio of the initial value of the axes,  $x_o/z_o$ . The solid line represents the collapse velocity for an oblate spheroid ( $\alpha_1 = \alpha_2 > \alpha_3$ ) in the case  $L \neq 0$ ,  $\Sigma \neq 0$  and  $\nu = 3$ . The dotted and dashed lines plot the result of the same calculation but in the case  $\nu = 2.5$  and  $\nu = 2$ , respectively. The figure shows two trends:

- a) the collapse velocity is reduced with increasing initial flattening (increasing value of  $x_o$ ). For example for  $z_o/x_o = 0.44$  the collapse velocity is reduced to the Hubble velocity in the plane of the pancake ( $H_p r_p$ ), while in the case of more extreme flattening  $z_o/x_o = 0.125$ , the collapse velocity is reduced by a factor of  $\simeq 6$  with respect the previous value.
- b) the collapse velocity is reduced with increasing angular momentum acquired by the protostructure. As shown, the collapse velocity is progressively reduced when we go from  $\nu = 3$  peaks to  $\nu = 2$ .

In other words, the slowing down of the rate of growth of density contrast produces a lowering of the peculiar velocity in qualitative and quantitative agreement with Barrow & Silk (1981) and Szalay & Silk (1983).

The result obtained helps to clarify the controversy relative to the previrialization conjecture. According to this paper, it is surely true that taking account only of the shear,  $\Sigma$ , produces a shortening of the collapse time of non-spherical perturbations, in agreement with Hoffman (1986a) and Bertschinger & Jain’s collapse theorem. The question is that in the real collapse other effects have an important role, namely external tides and the effects of small scale substructure. Both Hoffman (1986a) and Bertschinger & Jain (1994) results are valid for a fluid element, which has no substructure by definition, while a small scale substructure produces a slowing down of the collapse at least in two ways:

- 1) encounters between infalling clumps and substructure internal to the perturbation (Antonuccio-Delogu & Colafrancesco 1994; Del Popolo & Gambera 1997; Del Popolo & Gambera 1999);
- 2) tidal interaction of the main proto-structure with substructure external to the perturbation (Peebles 1990; Del Popolo & Gambera 1998).

Moreover, it should be pointed out that, as more small-scale power is present the collapse of a perturbation may be slowed down in a way that could inhibit the effect of shear.

Differently from Bertschinger & Jain (1994), our model takes account of the angular momentum of the system, and then at least of the effects produced by the point 2) quoted above. Similarly to Bertschinger & Jain (1994), our model does not take account of the substructure internal to the system. This last is a natural limitation of the homogeneous ellipsoid



model: a homogeneous ellipsoid cannot represent the substructure of the object. We, however, recall that the same shortcoming was present in Peebles (1990) paper: in that paper the substructure was suppressed, since it adopted an homogeneous Poisson distribution of particles within the protocluster (Peebles 1990). This limit has the effect of underestimating the effect of previrialization, and in particular the value of the overdensity at virialization,  $\delta_v$  (Peebles 1990). In other words, the effects of the slowing down of the collapse obtained in this paper (similarly to that of Peebles (1990)) are surely smaller than that we shall find if we had used a system having internal substructure, as in the above point 1).

Before concluding, we want to spend a few words on the impact of the result of the paper on our view of structure formation.

The reduction of the rate of growth of overdensity and collapse velocity has several consequences on structures formation. To begin with, a first consequence is a change of the mass function, the two-point correlation function, and the mass that accretes on density peaks. In fact, as several times remarked, the angular momentum acquired by a shell centered on a peak in the CDM density distribution is anti-correlated with density: high-density peaks acquire less angular momentum than low-density peaks (Hoffman 1986b; R88). A greater amount of angular momentum acquired by low-density peaks (with respect to the high-density ones) implies that these peaks can more easily resist gravitational collapse and consequently it is more difficult for them to form structure. This results in a tendency for less dense regions to accrete less mass, with respect to a classical spherical model, inducing a *biasing* of over-dense regions toward higher mass.

As a result, the number of objects with  $\sigma \leq 1$  (i.e., large mass) is smaller, since now the collapse is slowed down, and the mass function is now much below the standard PS prediction (Del Popolo & Gambera 1999; Del Popolo & Gambera 2000; Audit et al. 1997). Even the two-point correlation function of galaxies and clusters of galaxies results strongly modified (see Del Popolo & Gambera 1999; Del Popolo et al. 1999; Peebles 1993).

## 6. Conclusions

We examined the evolution of non-spherical inhomogeneities in a Einstein-de Sitter universe, by numerically solving the equations of motion for the principal axes and the density of a dust ellipsoid. We took account of the effect of the mass external to the perturbation by calculating the angular momentum transferred to the developing proto-structure by the gravitational interaction of the system with the tidal field of the matter becoming concentrated in neighboring proto-structures.

We showed that for lower values of  $\nu$  ( $\nu = 2$ ) the growth rate enhancement of the density

contrast induced by the shear is counterbalanced by the effect of angular momentum acquisition. For  $\nu > 3$  the effect of angular momentum and shear reduces, and the evolution of perturbations tends to follow the behaviour obtained in the spherical collapse model. These results corroborate the previrialization conjecture because they show that asphericities and tidal torques slow down the collapse of the perturbation after the system detaches from the general expansion.

I would like to thank Prof. E. Recami, E. Nihal Ercan and D. Eisenstein for some useful comments and an anonymous referee whose suggestions helped us to considerably improve the quality of this paper.

Finally, I would like to thank Boğaziçi University Research Foundation for the financial support through the project code 01B304.

## REFERENCES

- Andriani, E. and Caimmi, R., 1994, *A&A*, 289, 1
- Antonuccio-Delogu, V. and Colafrancesco, S., 1994, *ApJ*, 427, 72
- Audit, E., Teyssier, R. and Alimi, J. M., 1997, *A&A*, 325, 439
- Bardeen, J.M., Bond, J.R., Kaiser N. and Szalay A.S., 1986, *ApJ*, 304, 15
- Barnes, J. and Efstathiou, G., 1987, *ApJ*, 319, 575
- Barrow, J.D. and Silk, J., 1981, *ApJ*, 250, 432
- Bernardeau, F., 1994, *ApJ*, 427, 51
- Bertschinger, E. and Jain, B., 1994, *ApJ*, 431, 486
- Bond, J.R. and Myers, S.T., 1993a, preprint CITA/93/27
- Bond, J.R. and Myers, S.T., 1993b, preprint CITA/93/28
- Catelan, P. and Theuns, T., 1996a, SISSA preprint, astro-ph/9604077
- Catelan, P. and Theuns, T., 1996b, SISSA preprint, astro-ph/9604078
- Chernin, A.D., 1970, *Soviet Phys. JETP Letters* 11, 210

- Davis, M., Peebles, P.J.E., 1977, ApJS, 34, 425
- Del Popolo, A. and Gambera, M., 1997, A&A, 321, 691
- Del Popolo, A. and Gambera, M., 1998, A&A, 337, 96
- Del Popolo, A., Gambera, M., 1999, A&A, 344, 17
- Del Popolo, A., Takahashi, Y., Kiuchi, H. and Gambera M., 1999, A&A, 348, 667
- Del Popolo, A., Gambera, M., Recami, E. and Spedicato, E., 2000, A&A, 353, 427
- Doroshkevich, A.G., 1970, Astrophysics 3, 320
- Doroshkevich, A.G., 1973, Astrophys. Lett. 14, 11
- Eisenstein, D.J. and Loeb, A., 1995, ApJ, 439, 520
- Engineer, S., Kanekar, N. and Padmanabhan, T., 1998, astro-ph/9812452
- Evrard, A.E., Crone, M.M., 1992, ApJ, 394, L1
- Fall, S. M., 1983, in Internal Kinematics and Dynamics of Galaxies, IAU Symposium 100, ed. Athanassoula E. (Dordrecht, Reidel)
- Frenk, C. S., 1987, in Nearly Normal Galaxies: from the Planck time to the present, ed. Faber S., (New York, Springer-Verlag)
- Hoffman, Y., 1986a, ApJ, 308, 493
- Hoffman, Y., 1986b, ApJ, 301, 65
- Hoffman, Y., 1989, ApJ, 340, 69
- Hoyle, F., 1949, in IAU and International Union of Theoretical and Applied Mechanics Symposium, p. 195
- Lokas, E.L., Juskiwicz, R., Bouchet, F.R. and Hivon, E., 1996, ApJ, 467, 1
- Monaco, P., 1995, ApJ, 447, 23
- Nariai, H., Fujimoto, M., 1972, Progr. Theor. Phys. 47, 105
- Peebles, P.J.E., 1969, ApJ, 155, 393
- Peebles, P.J.E., Groth, E.J., 1976, A&A, 53, 131

Peebles, P.J.E., 1980, The large scale structure of the universe, Princeton university press

Peebles, P.J.E., 1990, ApJ, 365, 27

Peebles, P.J.E., 1993 Principles of Physical Cosmology, Princeton University Press

Pichon, C. and Bernardeau, F., 1999, astro-ph/9902142

Ryden, B.S. and Gunn J.E., 1987, ApJ, 318, 15

Ryden, B.S., 1988, ApJ, 329, 589

Ryden, B.S., 1988b, ApJ, 333, 78

Sasaki, M. and Kasai, M., 1997, astro-ph/9711252

Szalay, A.S. and Silk J., 1983, ApJ, 264, L31

Villumsen, J.V. and Davis, M., 1986, ApJ, 308. 499

White, S.D.M. and Silk, J., 1979, ApJ, 231, 1

White, S.D.M., 1984, ApJ, 286, 38

Zel'dovich, Ya.B, 1970, Astr. Ap. 5, 84

Zel'dovich, Ya.B and Novikov, 1983, Relativistic Astrophysics, Vol. 2, The Structure and Evolution of the Universe (Chicago: University of Chicago Press)

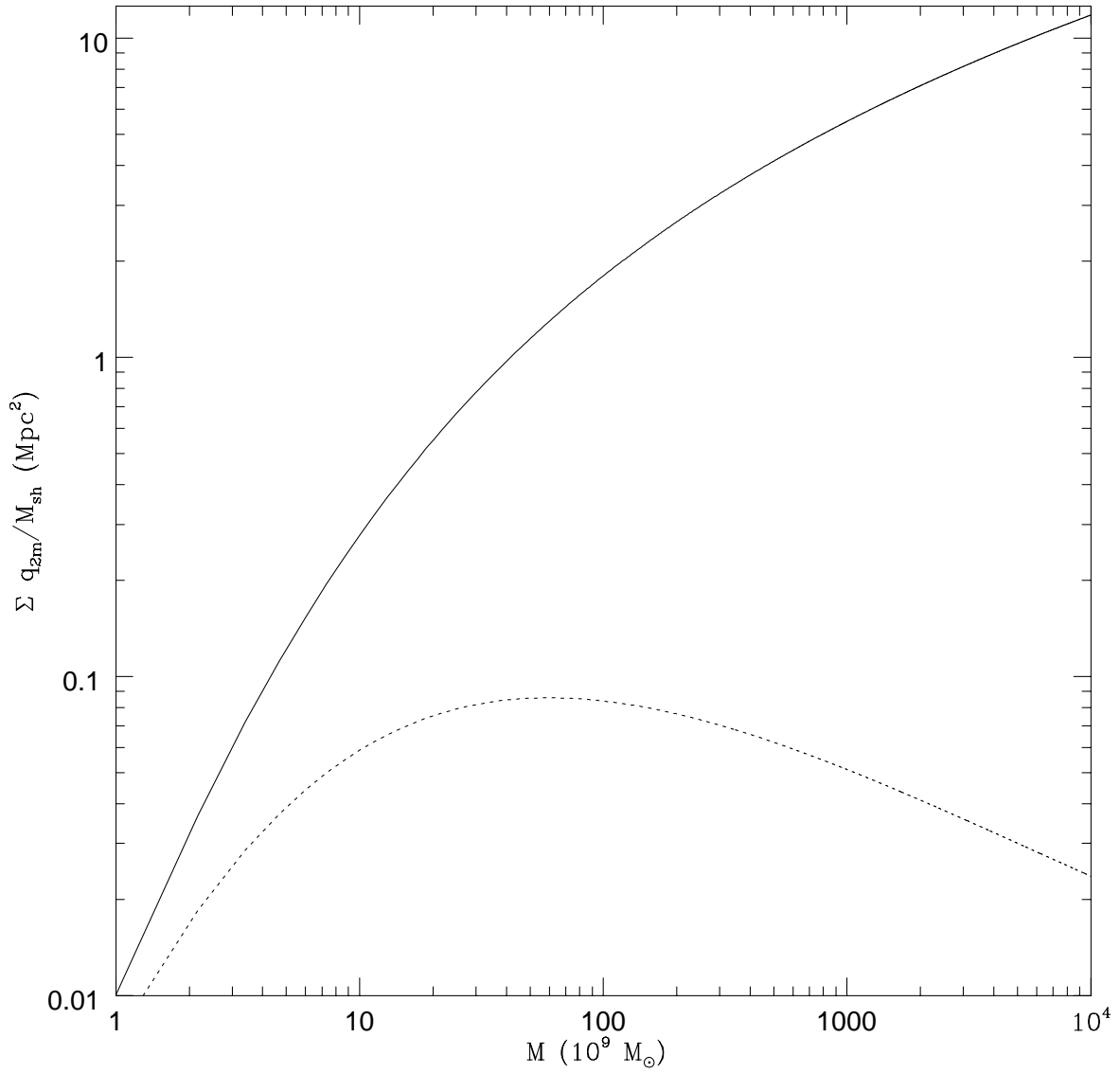


Fig. 1.— Comparison of the mean quadrupole moments due to triaxiality (dotted line), around a  $3\sigma$  peak, smoothed on galactic scale, with the sum of the r.m.s. quadrupole moments due to the secondary perturbations (solid line).

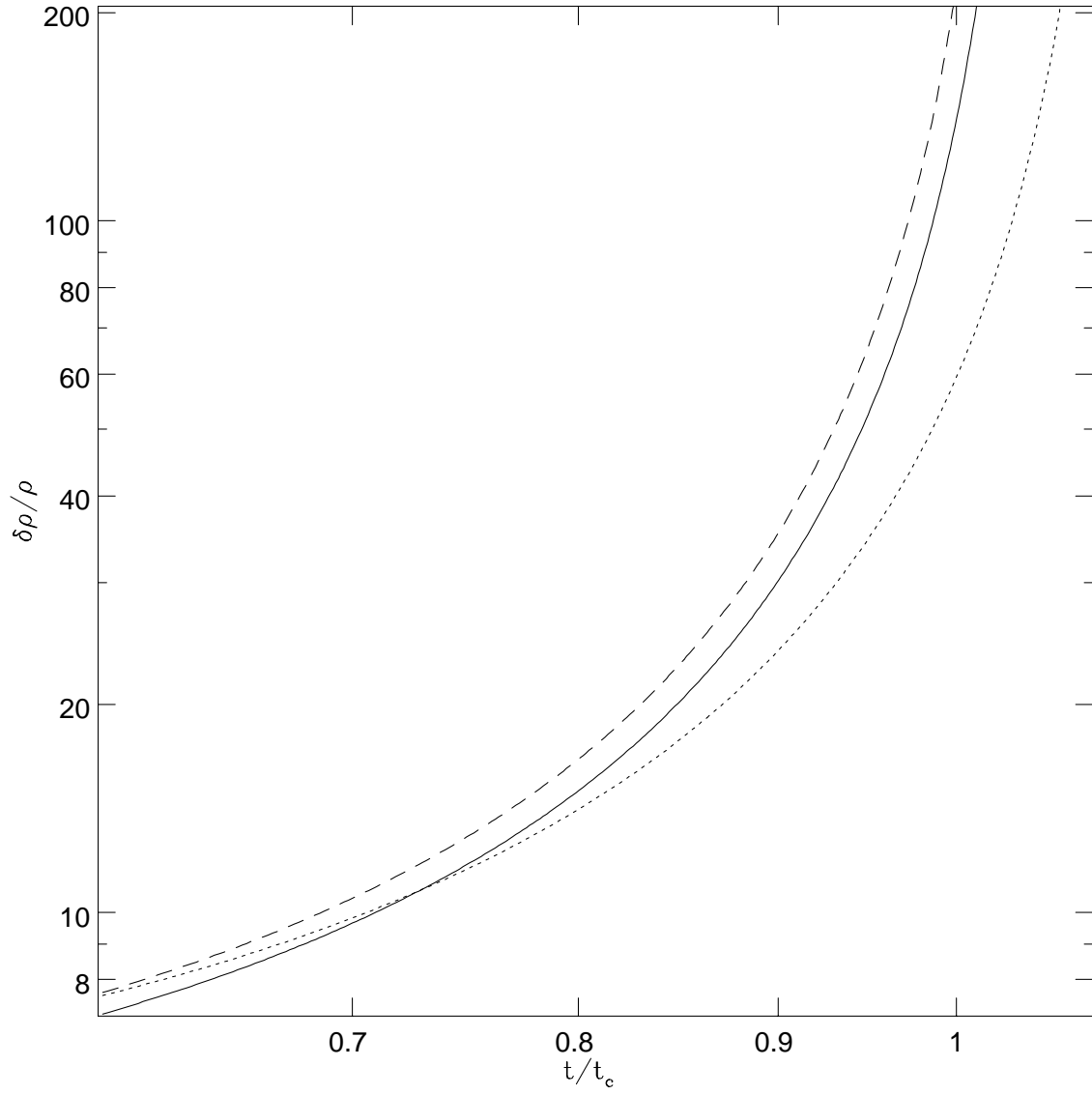


Fig. 2.— Evolution of ellipsoidal density perturbations in an expanding universe as function of redshift,  $z$ , for  $\nu = 2$  in the case  $L = \Sigma = 0$  (solid line),  $L = 0, \Sigma \neq 0$  (dashed line) and  $L \neq 0, \Sigma \neq 0$  (dotted line).

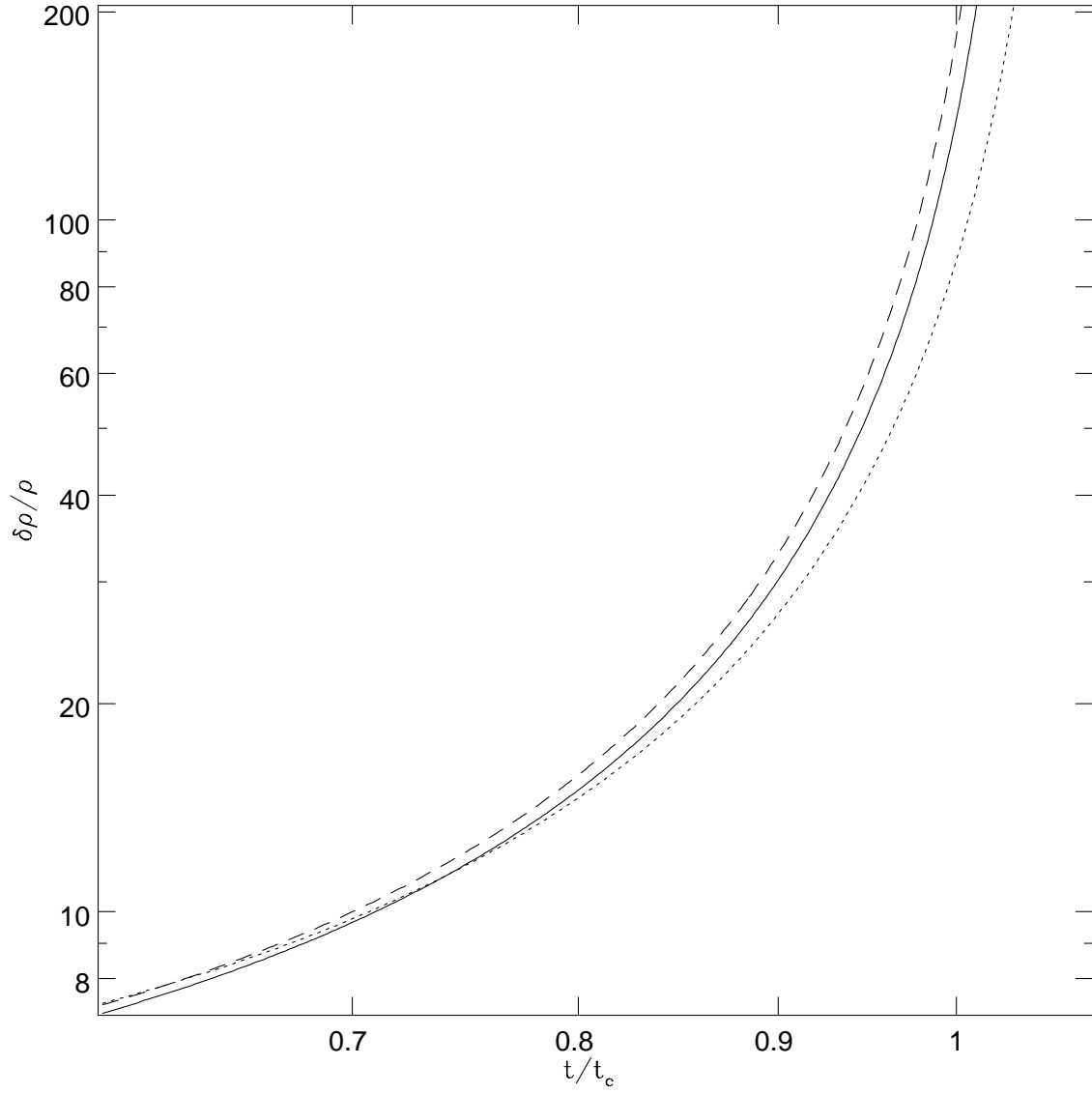


Fig. 3.— Same as figure 2 but now  $\nu = 2.5$ .

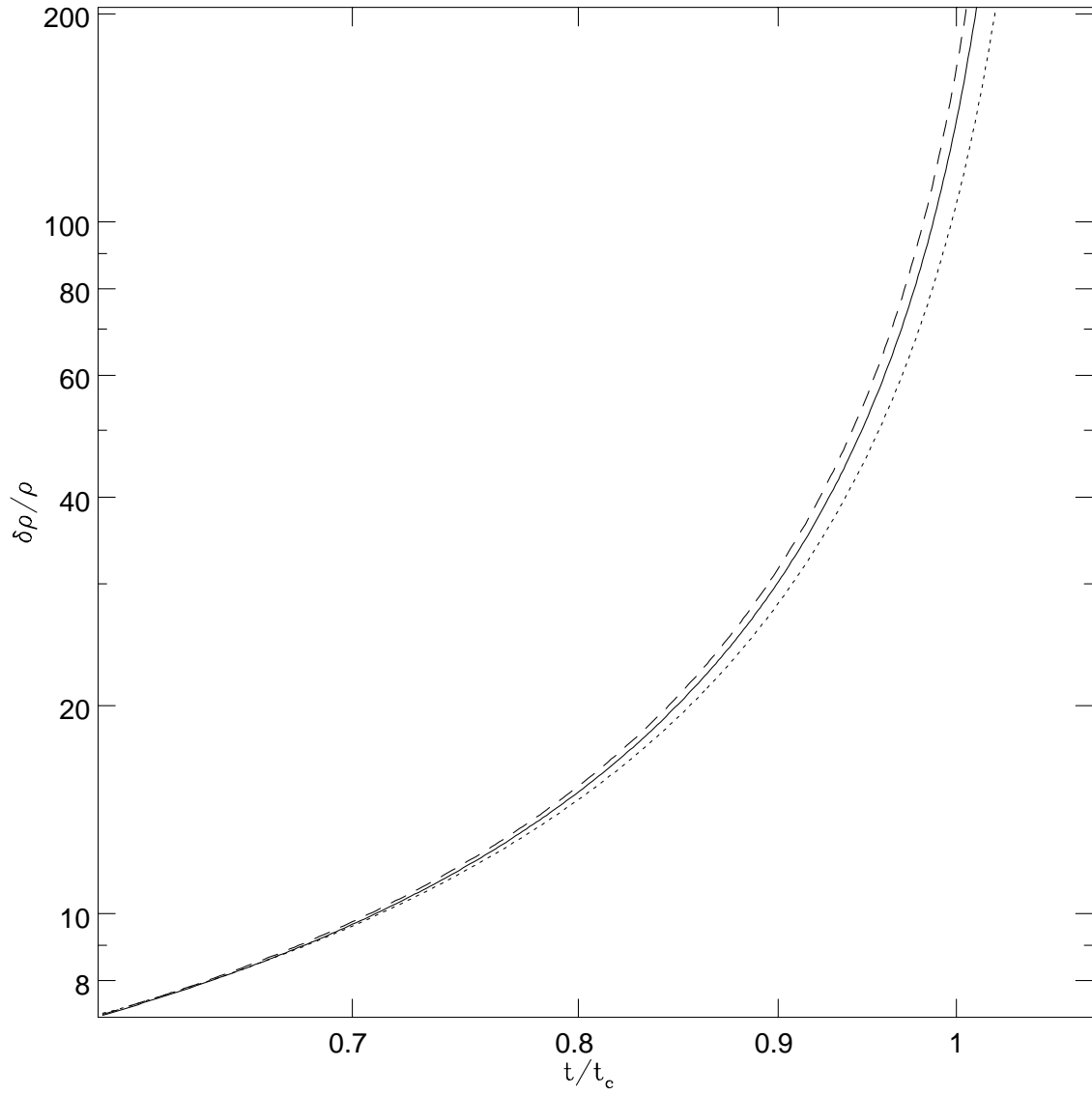


Fig. 4.— Same as figure 2 but now  $\nu = 3$ .



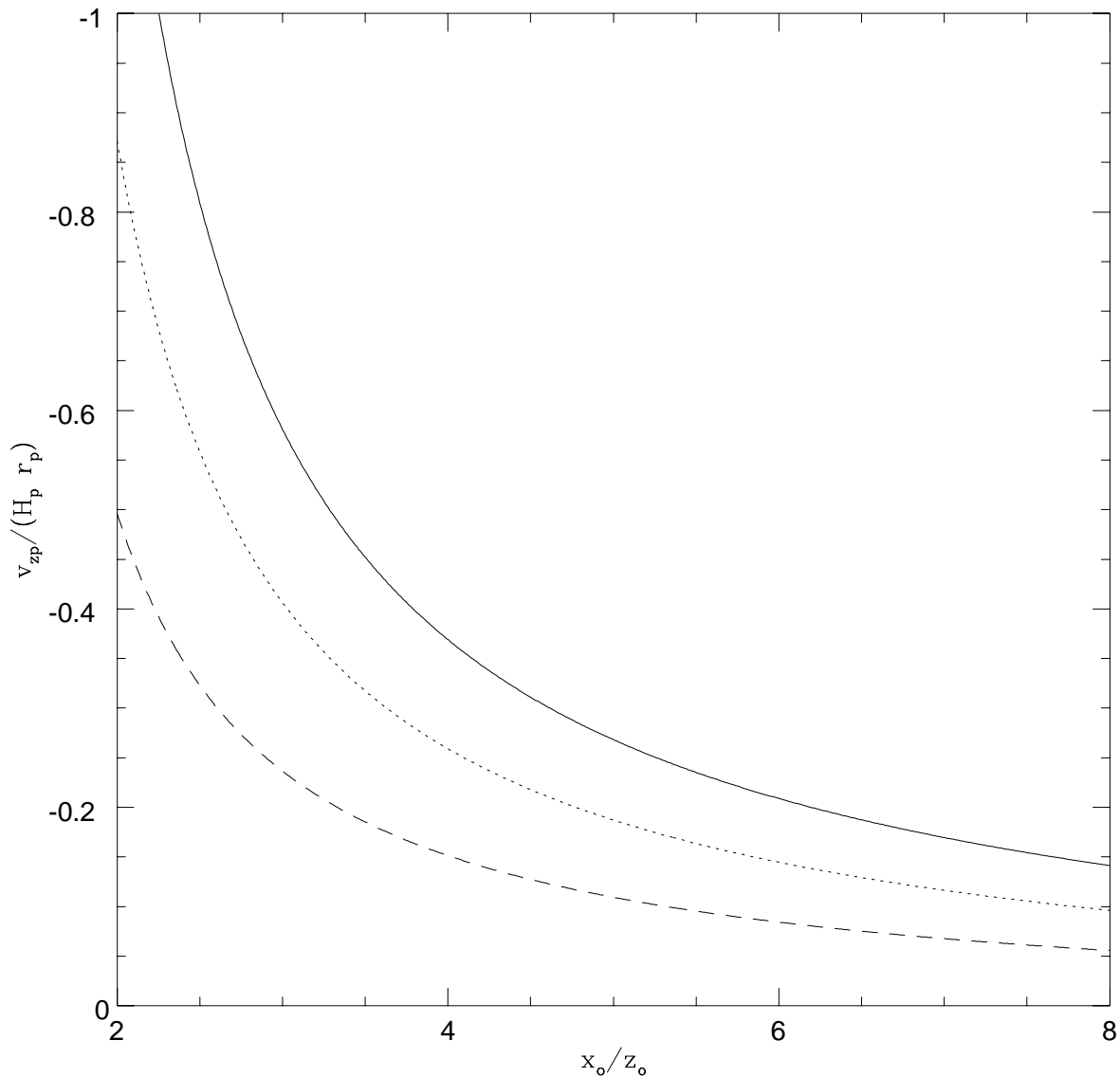


Fig. 5.— Collapse velocity for an oblate spheroid ( $\alpha_1 = \alpha_2 > \alpha_3$ ) down the  $z$  axis at epoch of pancaking (p).  $x_o$  and  $z_o$  are the initial values of the longest ( $x$ ) and shortest axis ( $z$ ),  $H_p$  and  $r_p$  are respectively the Hubble constant and the pancake radius at the pancaking epoch. The solid line represents the collapse velocity in the case  $L \neq 0$ ,  $\Sigma \neq 0$ , and  $\nu = 3$ . The dotted and dashed line the same calculation but for  $\nu = 2.5$ ,  $\nu = 2$ , respectively.